Kinetic study of the thermal decomposition of poly(vinyl alcohol)/kraft lignin derivative blends

D.M. Fernandes, A.A. Winkler Hechenleitner, E.A. Gómez Pineda *

Departamento de Química, Universidade Estadual de Maringá, Av. Colombo 5790, 87020-900 Maringá, PR, Brazil

Abstract

A kraft lignin derivative (KLD) obtained by reaction with *p*-aminobenzoic acid/phthalic anhydride, was blended with poly(vinyl alcohol) (PVA) by solution casting from DMSO. PVA and PVA/KLD films were exposed to ultraviolet radiation (Hg lamp, 96 h) and analyzed by thermogravimetry (TG) in inert and oxidative atmosphere. Typical multi-step decomposition profiles were obtained. The apparent activation energy (E_a) of the thermal degradation of the samples was computed by the Vyazovkin method. The KLD degradation presented only small intervals of decomposition degree with constant E_a values. PVA and blends showed intervals of up to 50% in decomposition degree with nearly constant E_a, and smaller intervals in which E_a varies drastically. The influences of samples irradiation and of surrounding gas in TG analysis on E_a are also shown.
© 2005 Elsevier B.V. All rights reserved.

1. Introduction

Studies on the use of different types of lignin, as additive or component in polymeric materials, have revealed that it can be useful acting for example as conductivity modifier [1], crosslinker [2], antioxidant/stabilizer [3–5], and others. In our previous work [6,7] interesting results of thermal properties were observed blending lignin with polyvinylalcohol (PVA). Lignin provides a protective effect towards thermal and photochemical degradation of PVA. The objective of this work was to continue and amplify the study of that system using a lignin derivative where *p*-aminobenzoic acid (PABA) was linked to the lignin molecules [8] which selection was based in the protective properties of PABA towards ultraviolet radiation [9]. Our interest in this work was to analyze the kinetic behavior during thermal decomposition of the pure polymers and blends using an isoconversional approach because it allows unmistakably detecting multistep kinetics [10–15]. Through such method, E_a is determined as a function of the degree of advance of the reaction, which reveals the complexity of the reaction in the overall interval of decomposition. The thermal degradation reaction was

studied in inert atmosphere (as in the former work) and also in oxidant atmosphere (synthetic air), because of its similarity with the ambient conditions. The Vyazovkin isoconversional method [10] was used in the kinetic study and FT-IR spectra of the volatile products and solid residues, at different reaction advances, were also analyzed.

2. Experimental

2.1. Reagents and chemicals

Poly(vinyl alcohol) 98–99% hydrolyzed, MW 13.000–23.000, was purchased from Aldrich. Lignin was isolated from kraft pulping black liquor [7] provided by Klabin, Paraná State, Brazil. A lignin derivative (KLD) was synthesized through reaction of the acetone insoluble fraction of a kraft lignin with the product of the reaction between phthalic anhydride and *p*-aminobenzoic acid. The synthesis reaction and the characterization of the KLD product is described elsewhere [8]. All other reagents had at least 99% purity.

2.2. Methods

Solutions of KLD and PVA in DMSO were prepared and proper volumes were mixed to prepare blends by casting, with

---

* Corresponding author. Tel.: +55 44 3261 4451; fax: +55 44 3263 5784.
  E-mail address: eagpineda@uem.br (E.A.G. Pineda).

compositions that allow film formation (not higher than 25% of KLD). The films were irradiated with an Hg vapor lamp with 48 mJ s^{-1} m^{-2} of fluence rate, that is, a normal street lamp at 15 cm from the sample where the local temperature do not exceeds 40 °C.

FT-IR spectra were performed on an FT-IR Bomem MB 100 spectrometer with samples prepared in 1% KBr pellets, with precision of 4 cm^{-1} in the peaks absorption.

DSC was performed on Shimadzu DSC-50 under flowing nitrogen (20 ml/min) atmosphere at 10 °C/min. Sample of 6 mg was placed into aluminum pan.

Thermogravimetric measurements were performed on a Shimadzu TGA 50 instrument, operating in dynamic mode under either flowing nitrogen (20 ml/min) or synthetic air (50 ml/min) atmosphere at heating rates of 2.5, 5, 10 and 20 °C/min. Samples of 6 mg and platinum pans were used. The TG curves obtained at different heating rates provided data for apparent activation energy computation through the Vyazovkin method [10] as summarized bellow. A number of about 400 points were used for the isoconversional plot and for the computations and graphic constructions a Microsoft Excel® Spreadsheet was constructed.

Simultaneous TGA-FT-IR analyses were carried out in a TG Netzsch-209 thermobalance and an FT-IR Bruker-Vector 22 spectrometer. Sample mass of 6–10 mg, flowing nitrogen and synthetic air of 20 ml/min and heating rate of 10 °C/min were used in these experiments.

2.3. Kinetic procedure

For the thermal decomposition of the solid, it was assumed that the reaction rate can be described as

$$\frac{d\alpha}{dt} = k_0 \, e^{-E_\alpha/RT} f(\alpha) \qquad (1)$$

where $d\alpha/dt$ is the reaction rate, E_α the activation energy as function of the degree of conversion (α), $f(\alpha)$ a function dependent on the reaction model, k_0 the rate constant at infinite temperature, T the temperature and R is the gas constant.

Under nonisothermal conditions in which a sample is heated at a constant rate, the explicit temporal dependence in Eq. (1) is eliminated through the trivial transformation:

$$\frac{d\alpha}{dT} = \frac{1}{\beta} k(T) f(\alpha) \qquad (2)$$

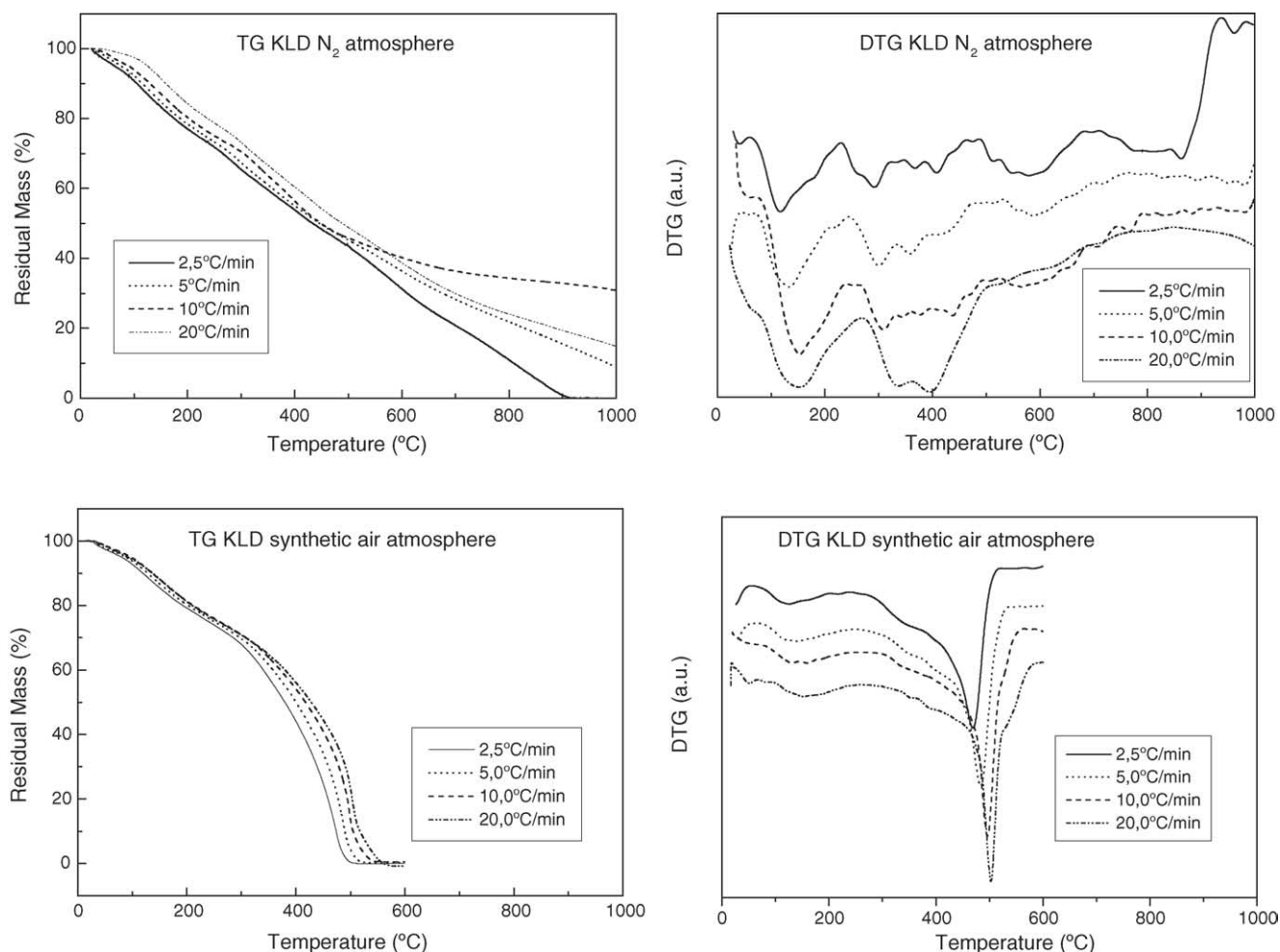β is the constant heating rate, $\beta = dT/dt$ and $k(T) = k_0 \, e^{-E/RT}$.

Fig. 1. TG and DTG curves for KLD. Experimental conditions: heating rate 10 °C/min and (a) nitrogen atmosphere and (b) synthetic air atmosphere.

Reordering Eq. (2), it can be written as

$$\frac{1}{f(\alpha)}\,d\alpha = \frac{k_0}{\beta}\,e^{-E/RT}\,dT \tag{3}$$

Integrating Eq. (3) between the limits $\alpha = 0$ and $\alpha = \alpha$ and the corresponding temperatures $T = T_0$ and $T = T$:

$$g(\alpha) = \frac{k_0}{\beta}\int_{T_0}^{T} e^{-E/RT}\,dT \tag{4}$$

If $E_a/2RT \gg 1$, Eq. (4) can be rounded to

$$g(\alpha) \approx \frac{k_0}{\beta}\frac{R}{E}T^2\,e^{-E/RT} \tag{5}$$

Arranging Eq. (5) and taking ln, we obtain

$$\ln\frac{\beta}{T_\alpha^2} = \ln\left[\frac{Rk_0}{E_\alpha g(\alpha)}\right] - \frac{E_\alpha}{R}\frac{1}{T_\alpha} \tag{6}$$

Eq. (6) can be used to calculate the associated activation energy E_α for every conversion if at least three dynamic measurements with different heating rates are available. To use the applied kinetics (simulation, conversion plot, isoconversion plot), this new formulation requires no knowledge of the reaction model ($f(\alpha)$ or $g(\alpha)$). With these new kinetics, selection a priori of the model with all its associated errors is no longer necessary. This leads to improved results as experience has shown that the known models correctly mirror reality only in isolated cases [10,14].

3. Results and discussion

The TG curve of KLD obtained in nitrogen and in synthetic air with the corresponding first derivative curve is shown in Fig. 1. The apparent activation energy (E_a) throughout the thermal decomposition reaction is presented in Fig. 2. At the first stage of the degradation of KLD in nitrogen atmosphere, a relatively well-defined DTG peak emerges, and from 250 °C on, only overlapped peaks occur, indicating a number of parallel and/or consecutive reactions. This behaviour is related to the heterogeneous structure of lignin. In air, two well-defined thermal decomposition stages are observed in the DTG curve, that is, an intense peak with a minimum at 498 °C and another rather weak peak at 150 °C. The larger number of reaction steps in N_2 is also evident in the plot of E_a versus % of decomposition. In nitrogen, there are only very short intervals in which E_a is constant, showing three maximum and four minimum values varying between 13 and 54 kJ/mol. On the other hand, in air, two maximum and three minimum E_a values are observed in the 95–230 kJ/mol interval and a near constant E_a of 150 kJ/mol between 43 and 60% of decomposition. It is important to note that thermal decomposition is favored in oxygen-containing atmosphere and that the E_a is as much as 100 kJ/mol higher than in inert atmosphere at a degree of decomposition higher than 15%.

The FT-IR spectra of the volatile and solid products of the thermodecomposition of KLD in inert and oxidative atmosphere are shown in Fig. 3. The 2350–2360 and 667 cm^{-1} peaks in Fig. 3(a and b, volatile products) are evidences of CO_2 formation. The intensity of these peaks is higher in inert (Fig. 3a)
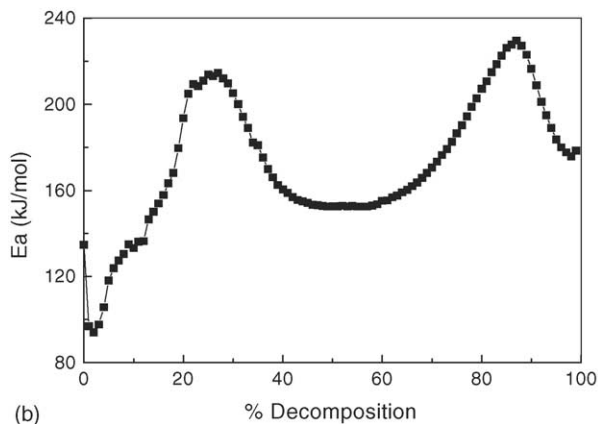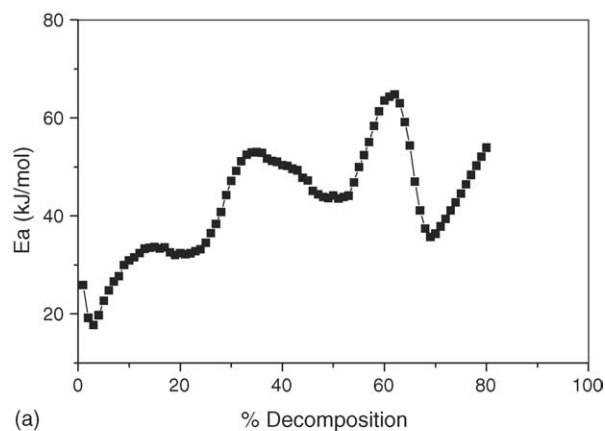

Fig. 2. E_a of the thermal degradation reaction of KLD: (a) in nitrogen and (b) in synthetic air atmosphere.

than in oxygen (Fig. 3b) containing atmosphere and increase directly with temperature, indicating an increase in CO_2 concentration. The weaker signals in the 3100–3700 cm^{-1} region in also indicate the occurrence of hydroxyl-containing products. CO characteristic peaks at 2100 and 2200 cm^{-1} and aromatic groups characteristic peaks in the 900–1000 cm^{-1} region are only visible in oxidant atmosphere. These reactions, that not occur in inert atmosphere, should be related to the higher values of E_a obtained in oxidant atmosphere (Fig. 2). Mazumder et al. [16] analyzed the volatile product of lignin pyrolysis through mass spectrometry and gaseous chromatography and detected various syringyl and guaiacyl structures such as guaiacol, syringol, eugenol, vanillin, sinapylic alcohol, coniferaldehyde, syringaldehyde, etc.

The FT-IR spectrum of the solid products of the same reaction at various degrees of reaction advance in inert and oxidative atmosphere is presented in Fig. 3c and d, respectively. In Fig. 3c, it can be observed a decrease in the O–H and C–H characteristic peaks (2800–3400 cm^{-1}) and changes in the carbonyl and aromatic peaks (1500–1700 cm^{-1}) during reaction. From 450 °C on, the 1700 cm^{-1} peak decreases significantly, and the 1500 cm^{-1} peak disappears while 1600 cm^{-1} peak increases. The 600–1250 cm^{-1} region shows that at 600 °C the solid residue is most probably a major proportion of char. In synthetic air atmosphere (Fig. 3d) it is also observed a decrease in
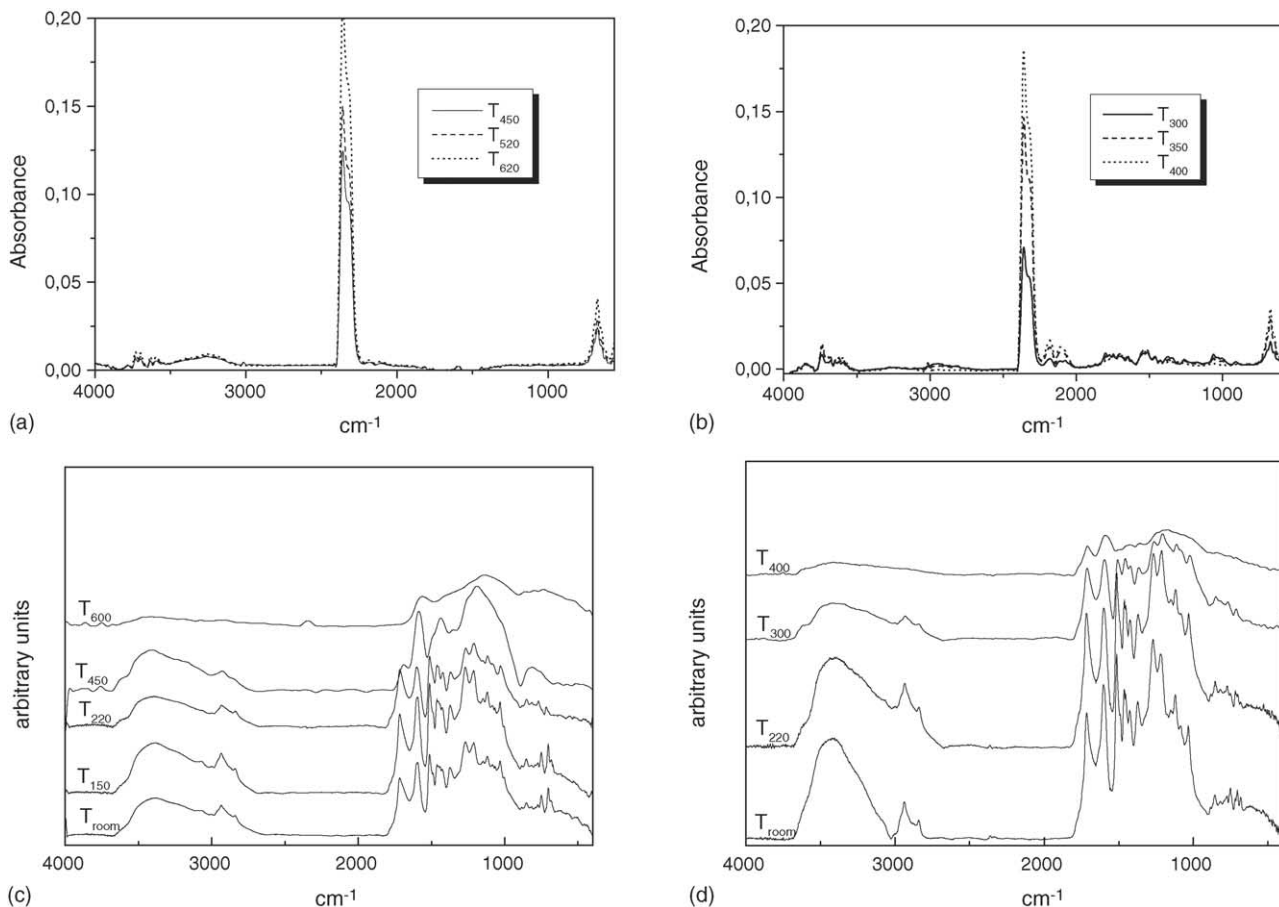
Fig. 3. FT-IR spectra of the KLD thermal decomposition products in N_2 atmosphere ((a) and (c)) and synthetic air atmosphere ((b) and (d)). Volatile products ((a) and (b)) and solid residues ((c) and (d)).

the O–H and C–H characteristic peaks and changes in the carbonyl and aromatic peaks (1500–1700 cm^{-1}) during reaction. Peaks in the 700–750 cm^{-1} region (1,4-disubstituted aromatic rings) are no longer visible at 400 °C. According to Ciobanu et al. [17], residues of the thermo-oxidative decomposition of lignin can be phenols and alkyl-radicals formed by the cleavage of the α–β-alkyl-aryl-ether linkages.

The KLD lignin derivative was blended with PVA in DMSO solution. PVA and PVA/KLD films were exposed to UV radiation of an Hg lamp for 96 h. Thermogravimetric analysis of irradiated and non-irradiated samples was performed in inert and in oxidative atmosphere. The ambient conditions are better represented by the oxidative atmosphere and it is of great importance to investigate how polymeric materials behave in such conditions, especially when practical applications are considered. The PVA thermograms are shown in Fig. 4. Comparing these TG curves obtained in nitrogen with those obtained in air, it can be seen that in air the reaction finishes at 520 °C, while in nitrogen it proceeds up to 800 °C. The DTG curves show significant differences. In nitrogen, only one intense and symmetric peak centered at 280 °C is observed together with other weak peaks throughout the reaction. In air, the DTG peak at 280 °C is large and has medium intensity. At least three peaks are overlapped, which indicates more reaction steps in this temperature range. The largest difference between the reactions in

both atmospheres is evidenced by a fine intense and symmetric DTG peak at the final stage of the reaction in air, in the range of 460–520 °C. Few differences are observed in these analyses between irradiated and non-irradiated samples.

As in the case of PVA, PVA/KLD blends show TG curves that strongly depend on the surrounding gas in the final stage of the thermal degradation. The DTG curves of the blends, irradiated and non-irradiated (not shown), are similar to that of the pure PVA shown in Fig. 4.

The apparent activation energy (E_a) of the thermal degradation reaction of PVA and the films of blends PVA/KLD 100/0, 85/15, and 75/25 in inert and in oxidative atmosphere was computed by the Vyazovkin isoconversional method (results in Fig. 5). In nitrogen, E_a shows low values up to 10% of decomposition for both irradiated and non-irradiated blend films. This fact is related to the presence of KLD because it shows E_a values of the same order of magnitude at the initial stage of decomposition. Such low E_a are attributed to low energy processes such as the elimination of low molar mass compounds (CO_2, H_2O, etc.) [18]. In the 15 to 60% interval of decomposition, all samples showed nearly constant E_a, ranging from 120 to 170 kJ/mol and slight increments due to sample irradiation and also due to KLD incorporation. For decomposition degree higher than 60%, E_a values show great oscillations even to negative values. The non-irradiated 75/25 blend is the only one that presents only positive
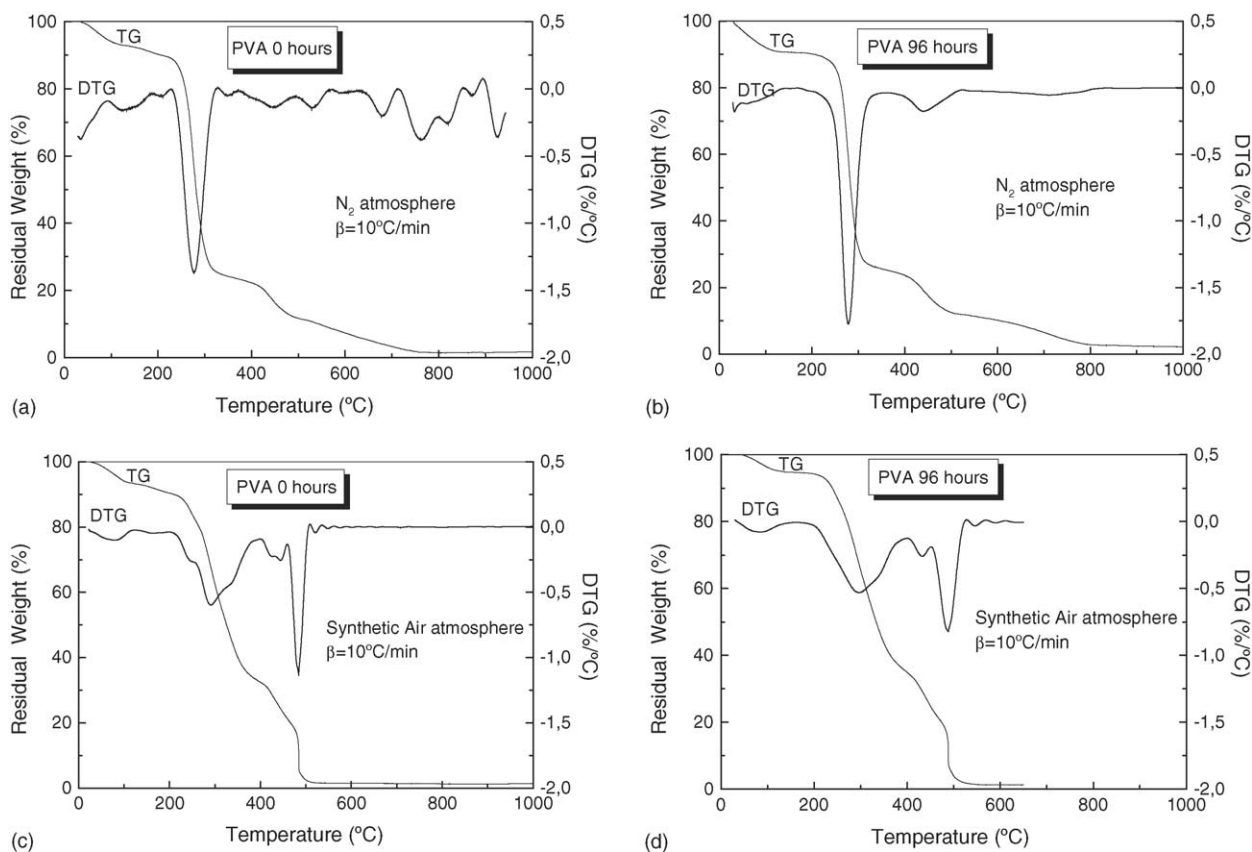
Fig. 4. Influence of the irradiation of PVA films and of atmosphere on thermogravimetric analysis.
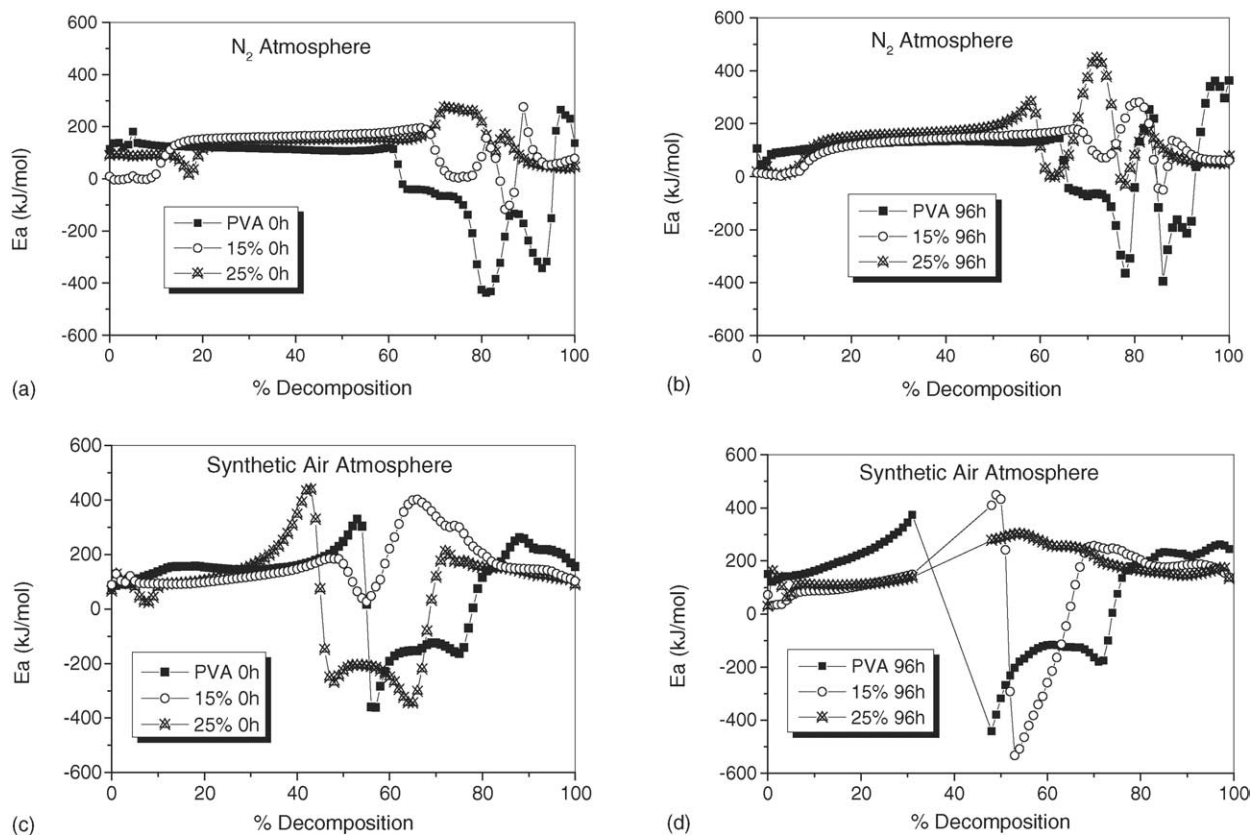

Fig. 5. Influence of the irradiation of PVA and PVA/KLD films and the termogravimetric analysis-atmosphere on E_a of thermal degradation reaction.
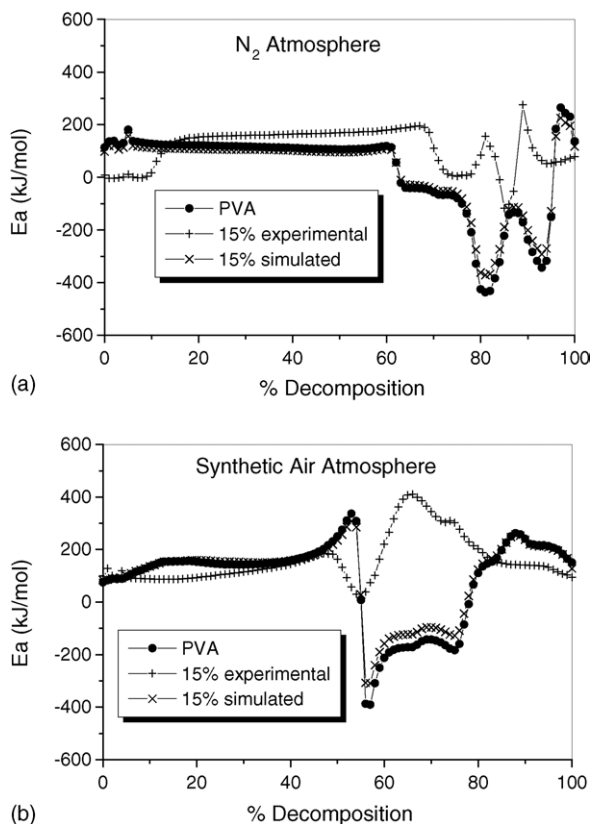
Fig. 6. Comparison of the real and the synthesized E_a vs. α curve for PVA/KLD 85/15, and also to the pure PVA: (a) N_2 atmosphere and (b) synthetic air atmosphere.

values. A nearly constant E_a is related with a unique reaction step or with a multi-step process controlled by the slowest step. Negative E_a values do not have physical significance and are most probably originated by complex parallel reactions involving free radicals [18,19].

In synthetic air atmosphere, the non-irradiated samples (Fig. 5c) show nearly constant E_a (around 100–150 kJ/mol) up to 40–50% decomposition and large variations at higher reaction advances. In the case of irradiated samples, the curve profiles are similar, but the nearly constant E_a interval is smaller and E_a values are larger than those of non-irradiated films. E_a values lower than −600 kJ/mol were obtained in the 30–48% decomposition interval and they were removed from these curves.

The E_a versus decomposition degree curves were also synthesized by the addition of the two pure polymer curves, according to the blend composition. Fig. 6 shows the comparison of these simulated curves with the real ones for blend 15/85. The pure PVA curve was also included for comparison's sake. Because of the low LKD content, the simulated curves differ only very slightly from the pure PVA curve. In both inert and oxidative atmospheres, there are intervals in which the real curve dislocates significantly from the simulated one. A similar behavior was observed for other compositions. This result shows that the reactions that take place in the thermal decomposition of the blends are different from those that occur in the pure polymers, probably due to specific interactions between polar groups of the polymeric chains, as also suggested by another analysis [8].

The FT-IR spectra of the volatile products of the thermal decomposition of PVA and of the PVA/KLD 85/15 blend, in inert and oxidative atmosphere are shown in Fig. 7. In the case of PVA in N_2 (Fig. 7a), the spectrum with most intense signals is obtained when the sample undergoes 220 °C during the thermogravimetric analysis acquisition. These signals are characteristic of CO_2 (at 2350 cm^{-1}) and carbonyls (at 1715 cm^{-1}), most probably from volatile aldehydes. The less intense peaks observed at 2700–3000 cm^{-1}, may have been originated by water, alcohols and unsaturated compounds, which also originate signals in the 1000–1200 cm^{-1} region present in this spectrum. There is also a shoulder at 1760 cm^{-1} characteristic of saturated ketones. The peak at 1745 cm^{-1} in the spectrum of the volatile products corresponding to the sample temperature of 400 °C is most probably originated by unsaturated ketones [20]. Another peak at 1640 cm^{-1} may be related to water and/or C=C bonds of volatile alkenes. A different behavior was observed in the spectra of the PVA volatile products in synthetic air (Fig. 7c). The 1745 cm^{-1} peak undergoes a maximum intensity at 220 °C while the 2350 cm^{-1} peak increases with increasing temperature throughout the reaction. Pure PVA, until $\alpha = 0, 1$ ($T = 200$ °C), reacting in both atmospheres show similar FT-IR results (Fig. 7a and c), nevertheless in synthetic air the E_a is slightly lower (75–137 kJ/mol) than in nitrogen (115–180 kJ/mol), as observed in Fig. 5a and c. In nitrogen, from $\alpha = 0, 6$ ($T = 400–500$ °C) on, negative E_a values are obtained. In this stage of the reaction, exothermic processes take place as can be seen in the DSC analysis in Fig. 8.

The spectra of the gaseous pyrolysis products of the reaction of the PVA/KLD 85/15 blend in N_2 atmosphere (Fig. 7b) show that the signals attain a maximum intensity when the sample is heated to 600 °C (this happens at 220 °C for pure PVA). The peak wavenumbers and their most probable attributions are as follows: 3600–3750 cm^{-1} of hydroxyl-containing compounds; 2350 cm^{-1} of carbon dioxide; 1745 cm^{-1} of unsaturated ketones; 1705 cm^{-1} of unsaturated aldehydes and ketones; 1550 cm^{-1} of volatile alkenes and/or carboxylic acids. On one hand, it can be observed that the peak at 2350–2360 cm^{-1} is very similar to that of the KLD pyrolysis products (Fig. 3a), and on the other hand, the peaks present in the PVA pyrolysis products (Fig. 7a) are rather distinct. Based on these results, it can be said that the carbonylic products formed in the blend reaction are different from those formed in the pure PVA reaction. In the case of the blend reaction in oxidative atmosphere, carbonyl containing volatile molecules are practically absent and CO_2, detected by the 2350 cm^{-1} intense peak, is present at all stages of the reaction (see Fig. 7d).

Fig. 9 shows the FT-IR spectrum of the original samples (PVA and 85/15 blend) and the solid residues of the decomposition reaction in inert and oxidative atmosphere, at four reaction advance degrees Alterations in the intensity of various peaks are observed during reaction. In N_2, for PVA and blend (Fig. 9a and b) the intensity of the OH band (3000–3700 cm^{-1}) decreases, the peak maximum shifts to lower wavenumbers as the reaction proceeds, and the shoulder on the right side of the band (due to bonded OH) dessapears. The peaks in the range 2700–3000 cm^{-1} are practically absent at the final stage of the
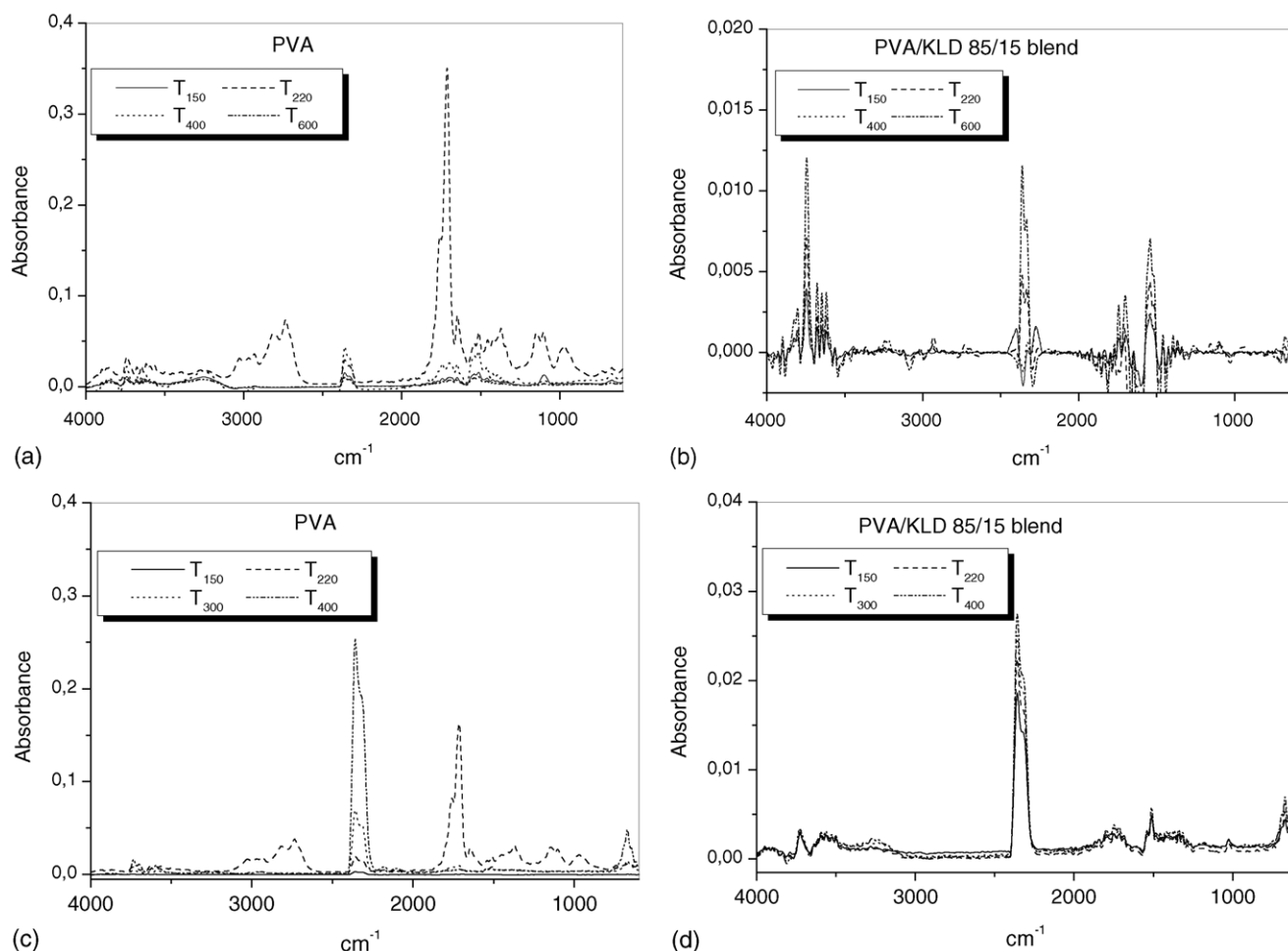
Fig. 7. FT-IR spectra of the volatile products of the thermal decomposition of PVA ((a) and (c)) and of the PVA/KLD 85/15 blend ((b) and (d)), in inert ((a) and (b)) and oxidative atmosphere ((c) and (d)).

reaction. In the $1550–1750\,\mathrm{cm^{-1}}$ range the signals are originated by the C=C, C=O and water molecules. The original samples show three signals in this interval and from $400\,^{\circ}\mathrm{C}$ on, only two peaks are visible, one at $1690\,\mathrm{cm^{-1}}$ (due probably to unsaturated ketones) and another more intense at $1580\,\mathrm{cm^{-1}}$ (characteristic of carboxylate ion). CH_2 vibrations, C–H, O–H
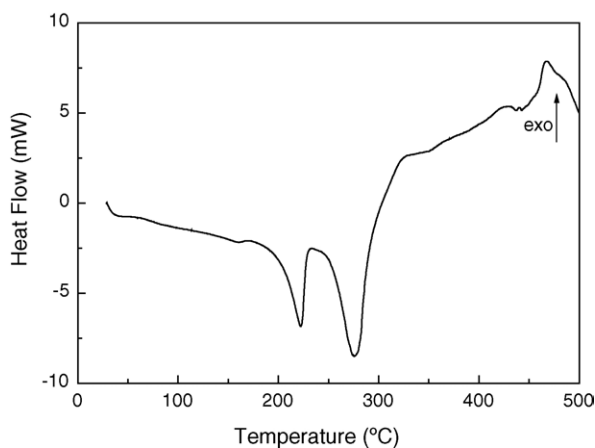

Fig. 8. DSC curve of PVA.

deformations and C–C and C–O stretchings originate peaks in the $1200–1500\,\mathrm{cm^{-1}}$ region. The C–C–C stretching band at $1143\,\mathrm{cm^{-1}}$ is attributed to PVA crystallinity [19]. From $220\,^{\circ}\mathrm{C}$ on, these absorption bands and the 916 and $815\,\mathrm{cm^{-1}}$ peaks (attributed to PVA tacticity) show a large decrease. In this way, it can be said that various carbonyl compounds such as ketones, carboxyl acids, and others may be formed. Furthermore, the presence of a low quantity of KLD in PVA films plays an important role in the thermal decomposition reaction as it results in char with major aromatic and hydroxyl groups content.

It is well known that alcohols dehydrate forming unsaturated compounds. In PVA pyrolysis, a first stage with the elimination of water and the formation of C=C bonds is proposed together with further complex reactions such as keto-enolic tautomerization, hydrogen transference, cross-linkages formation, cyclization, besides the formation of free radicals. Holland and Hay [21] reported that saturated and unsaturated aldehydes and ketones, vinyl esters and terminal alkynes are formed in PVA pyrolysis, while Gilman et al. [20] reported the formation of conjugated aliphatic and aromatic polyens, substituted cycloalkenes, and other unsaturated compounds. In spite of the similar behavior shown by the spectra of both samples up to $400\,^{\circ}\mathrm{C}$, the final products (at $600\,^{\circ}\mathrm{C}$) reveal different structures.
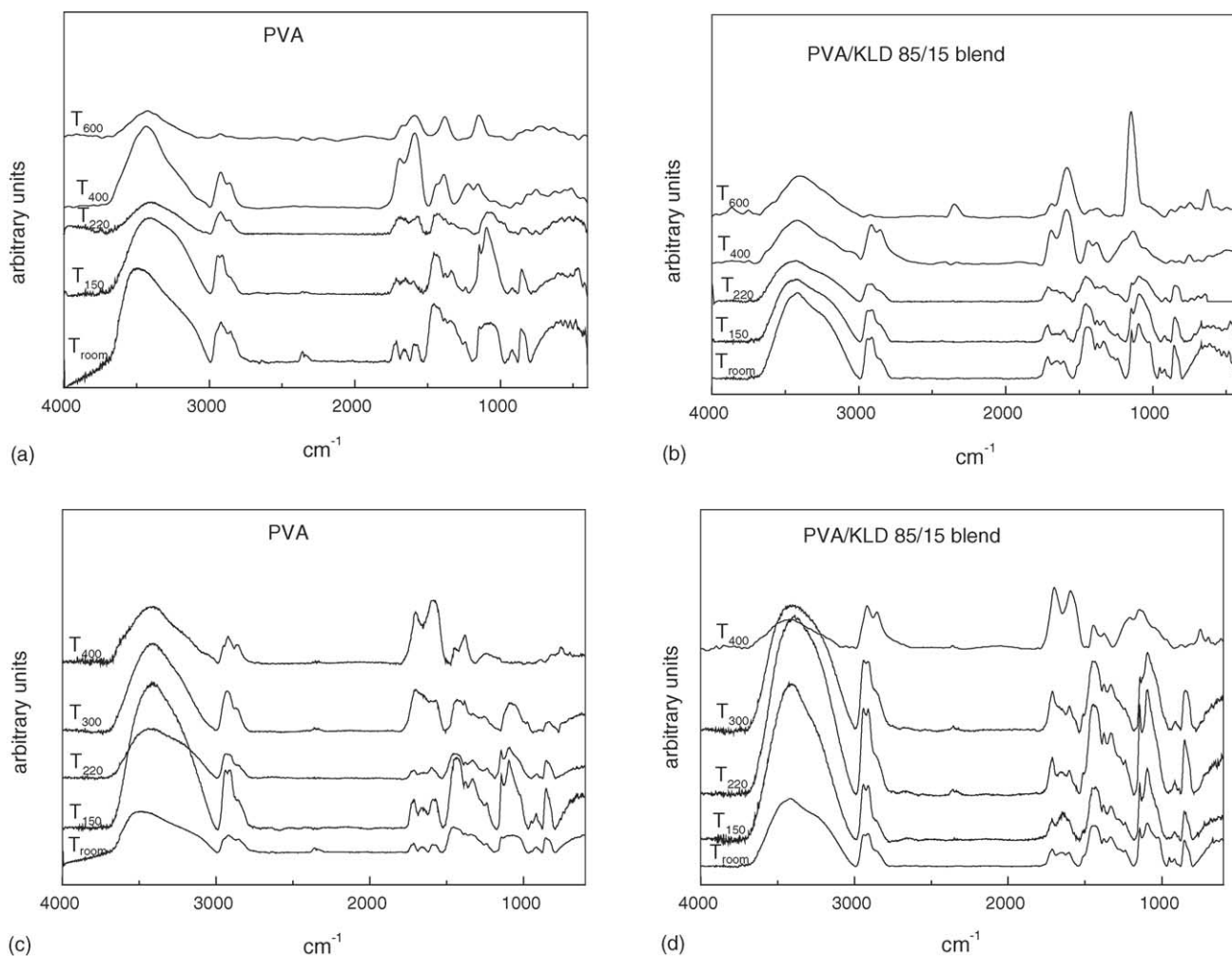
Fig. 9. FT-IR spectra of the solid products of the thermal decomposition of PVA ((a) and (c)) and of the PVA/KLD 85/15 blend ((b) and (d)), in inert ((a) and (b)) and oxidative atmosphere ((c) and (d)).

In synthetic air, it is observed that the carbonyl content in the solid product increases during the reaction, for both samples PVA and PVA/KLD blend. Another characteristic peaks observed in these spectra are of molecules containing saturated hydrocarbons (2800–3000 and 1000–1200 cm^{-1}), aromatic rings (1600 cm^{-1}) and hydroxyles (3000–3700 cm^{-1}).

4. Conclusions

The thermal decomposition reaction of KLD, PVA and PVA/KLD blends (containing up to 25% KLD) finishes at lower temperatures in air than in nitrogen atmosphere. TG/DTG analysis of these samples also shows that the number of thermal decomposition reaction steps is strongly dependent on the surrounding gas. Irradiated and the corresponding non-irradiated samples show similar TG/DTG curves.

The E_a versus decomposition degree curves reveal that complex reactions occur in both atmospheres, showing only small intervals with nearly constant E_a values (KLD) or large oscillations even with negative values (PVA and PVA/KLD blends). For these reasons, a model-fitting method is not applicable in the overall reaction interval of these polymers. E_a values for the

decomposition reactions in air are larger than those in nitrogen. In general, PVA/KLD blends initiate reaction with very low E_a, similarly to KLD. From nearly 10% (decomposition) on, the E_a of the thermal decomposition of PVA in N_2 shows only small variations due to irradiation and KLD incorporation. In air, the E_a of PVA increases (up to 30% decomposition) when the film is irradiated and the effect is minimized in KLD-containing PVA films.

The FT-IR spectra of the volatile products and the solid residue formed in the thermal decomposition of PVA and PVA/KLD show that very different reactions take place in these samples. It can be said that the presence of a low quantity of KLD in PVA films plays an important role in the thermal decomposition reaction, providing a char with major aromatic and hydroxyl groups content.

References

[1] P.C. Rodrigues, M.P. Cantao, P. Janissek, P.C. Scarpa, A.L. Mathias, L.P. Ramos, M.A.B. Gomes, Eur. Polym. J. 38 (2002) 2213.
[2] V.E. Gul, E.G. Lyubeshkina, A.M. Shargorodskii, Mekhanika Polym. 1 (1965) 3.
[3] K. Levon, J. Huhtala, B. Malm, J.J. Lindberg, Polymer 28 (1987) 745.

[4] B. Kosikova, V. Demianova, M. Kacurakova, J. Appl. Polym. Sci. 47 (1993) 1065.

[5] R. Pucciariello, V. Villani, C. Bonini, M. D'Auria, T. Vetere, Polymer 45 (2004) 4159.

[6] E. Corradini, E.A.G. Pineda, A.A.W. Hechenleitner, Polym. Degrad. Stab. 66 (1999) 199.

[7] P.R.S. Bittencourt, G.L. dos Santos, E.A.G. Pineda, A.A.W. Hechenleitner, J. Therm. Anal. Cal. 79 (2005) 371.

[8] D.M. Fernandes, A.A.W. Hechenleitner, A.E. Job, E. Radovanovic, E.A.G. Pineda, Polym. Deg. Stab., in press.

[9] M.L. Hu, Y.K. Chen, L.C. Chen, M. Sano, Nutr. Biochem. 6 (1995) 504.

[10] S. Vyazovkin, C.A. Wight, Thermochim. Acta 340/341 (1999) 53.

[11] H. Friedman, J. Polym. Sci. 6 (1963) 183.

[12] T. Ozawa, Bull. Chem. Soc. Jpn. 38 (1965) 1881.

[13] J.H. Flynn, L.A. Wall, J. Res. Nat. Bur. Stand. 70a (1996) 487.

[14] Mettler Toledo Gmbh Analytical: Model Free Kinetics. http://www.mt.com/ta.

[15] J.P. Haines, Thermal methods of analysis: principles, applications and problems, Blackie Acad. Profess. (1995) 30.

[16] B. Mazumder, A. Nakgawa, K. Kuroda, Y. Ohtani, K. Sameshima, Ind. Crops Prod. 21 (2005) 17.

[17] C. Ciobanu, M. Ungureanu, L. Ignat, D. Ungureanu, V.I. Popa, Ind. Crops Prod. 20 (2004) 231.

[18] K. Pielichowski, Solid State Ionics 104 (1997) 123.

[19] M. Shibayama, T. Yamamoto, C.F. Xiao, S. Sakurai, A. Hayami, S. Nomura, Polymer 32 (6) (1991) 1010.

[20] T.W. Gilman, L. David, H. Vander, K. Takashi, in: Proceedings of the ACS Symposium Series 599, Washington, DC, August 21–26, J. Am. Chem. Soc. (1994).

[21] B.J. Holland, J.N. Hay, Polymer 42 (2001) 6775.